



Providing Choice & Value
Generic CT and MRI Contrast Agents

**FRESENIUS
KABI**

CONTACT REP

AJNR

**Arterial Spin-Labeling MR Imaging for the
Differential Diagnosis of
Venous-Predominant AVMs and
Developmental Venous Anomalies**

D.H. Yoo, C.-H. Sohn, H.-S. Kang, Y.D. Cho and K.M. Kim

This information is current as
of July 8, 2025.

AJNR Am J Neuroradiol published online 29 June 2023
<http://www.ajnr.org/content/early/2023/06/29/ajnr.A7922>

Arterial Spin-Labeling MR Imaging for the Differential Diagnosis of Venous-Predominant AVMs and Developmental Venous Anomalies

 D.H. Yoo,  C.-H. Sohn,  H.-S. Kang,  Y.D. Cho, and  K.M. Kim



ABSTRACT

BACKGROUND AND PURPOSE: Venous-predominant AVMs are almost identical in appearance to developmental venous anomalies on conventional MR imaging. Herein, we compared and analyzed arterial spin-labeling findings in patients with developmental venous anomalies or venous-predominant AVMs, using DSA as the criterion standard.

MATERIALS AND METHODS: We retrospectively collected patients with either DVAs or venous-predominant AVMs, each available on both DSA and arterial spin-labeling images. Arterial spin-labeling imaging was visually assessed for the presence of hyperintense signal. CBF measured at the most representative section was normalized to the contralateral gray matter. The temporal phase of developmental venous anomalies or venous-predominant AVMs was measured on DSA as a delay between the first appearance of the intracranial artery and the lesion. Correlation between the normalized CBF and the temporal phase was evaluated.

RESULTS: Analysis of 15 lesions (13 patients) resulted in categorization into 3 groups: typical venous-predominant AVMs (temporal phase, <2 seconds), intermediate group (temporal phase between 2.5 and 5 seconds), and classic developmental venous anomalies (temporal phase, >10 seconds). Arterial spin-labeling signal was markedly increased in the typical venous-predominant AVM group, while there was no discernible signal in the classic developmental venous anomaly group. In the intermediate group, however, 3 of 6 lesions showed mildly increased arterial spin-labeling signal. The normalized CBF on arterial spin-labeling and the temporal phase on DSA were moderately negatively correlated: $r(13) = 0.66$, $P = .008$.

CONCLUSIONS: Arterial spin-labeling may predict the presence and amount of arteriovenous shunting in venous-predominant AVMs, and using arterial spin-labeling enables confirmation of typical venous-predominant AVMs without DSA. However, lesions with an intermediate amount of shunting suggest a spectrum of vascular malformations ranging from purely vein-draining developmental venous anomalies to venous-predominant AVMs with overt arteriovenous shunting.

ABBREVIATIONS: ASL = arterial spin-labeling; DVA = developmental venous anomaly; GKS = gamma knife surgery; nCBF = normalized CBF; SWAN = T2 star-weighted angiography; TCV = temporal phase in regard to the cortical vein (on DSA); TP = temporal phase (on DSA); vpAVM = venous-predominant AVM

Developmental venous anomaly (DVA) is the most frequently encountered cerebral vascular malformation, with a reported incidence of approximately 2%–3%. DVAs are usually incidentally detected and appear as a caput medusa or umbrella-like medullary veins collecting into a single common draining vein (stem vein).^{1,2} A venous-predominant AVM (vpAVM), a rare form of AVM, is almost identical in appearance to DVAs on conventional MR

imaging. This type of AVM has no definable nidus, and early venous drainage is the only feature that distinguishes it from a DVA.^{3,4} However, whereas a DVA is of little clinical significance, a vpAVM may cause venous hypertension or hemorrhage.^{4–6} Whether symptomatic or incidentally detected, a vpAVM is conventionally diagnosed through DSA, which poses a risk to patients because it is an invasive procedure involving iodinated contrast and radiation exposure.

Arterial spin-labeling (ASL) is a noninvasive MR imaging technique used to assess cerebral circulation by magnetically labeling inflowing blood.⁷ The availability and application of ASL have steadily increased, and its usefulness in evaluating arteriovenous shunting of intracranial AVMs is well-recognized.^{8,9} We hypothesized that ASL would effectively represent the presence and degree of shunting in vpAVM, thus enabling a diagnosis of vpAVM without the use of contrast or invasive DSA. SWI has

Received March 6, 2023; accepted after revision June 5.

From the Departments of Radiology (D.H.Y., C.-H.S., Y.D.C.) and Neurosurgery (H.-S.K., K.M.K.), Seoul National University Hospital, Seoul National University College of Medicine, Seoul, Korea.

Please address correspondence to Chul-Ho Sohn, MD, PhD, Department of Radiology, Seoul National University Hospital, Seoul National University College of Medicine, 101 Daehak-ro, Jongno-gu, Seoul, 03080, Korea; e-mail: neurorad63@gmail.com

 Indicates article with online supplemental data.

<http://dx.doi.org/10.3174/ajnr.A7922>

also been reported to serve as an accurate tool for detection of arteriovenous shunting.^{10,11} The purpose of the present study was to compare and analyze ASL and SWI findings in patients with DVA or vpAVM, using DSA as the criterion standard.

MATERIALS AND METHODS

Patient Selection

This study was approved by the local ethics review board; written informed consent was waived due to its retrospective nature. We searched the PACS data base at our center between January 2016 and December 2019 for MR images that included ASL sequences acquired from a 3T MR imaging system (Discovery 750; GE Healthcare). To screen patients for a DVA or vpAVM, we used keywords as follows: “developmental venous anomaly,” “DVA,” “venous angioma,” “arteriovenous malformation,” “AVM,” and “venous-predominant.” Next, we selected only those with available DSA images. Patients with coexisting disease that could hinder proper evaluation of the ASL signal were excluded. Medical records were reviewed to collect demographics and clinical data.

Image Acquisition

A multiphase ASL protocol was the most frequently used sequence in our institution, with the best image quality. Thus, we limited our series to those who underwent this protocol to ensure homogeneity of the study population. We applied the following parameters: TR/TE = 5871/11.0 ms; number of averages = 1; section thickness = 6 mm; number of slices = 26–28; readout = 4 spiral arms \times 640 samples; FOV = 240×240 mm²; matrix = 128×128 ; and voxel resolution = $3.8 \times 3.8 \times 6.0$ mm. Details of the technique used to acquire multiphase ASL images are described in a previous report.¹² Along with ASL, all patients were examined with T2 star-weighted angiography (SWAN). The SWAN parameters were TE = 21.5 ms; TR = 37.3 ms; flip angle = 300°; thickness = 1.2 mm; matrix = 416×256 ; FOV = 220×220 ; number of slices = 120.

DSA was performed on either an Innova IGS 630 (GE Healthcare) system or AlluraClarity (Philips Healthcare). After puncture of the femoral artery and insertion of a 5F arterial sheath, selective catheterization of the dominant vertebral artery and bilateral internal carotid arteries was performed. A bolus of 7–9 mL of contrast media was injected at an injection rate of 5–6 mL/s by a contrast delivery system. The image-acquisition frequency was in 3 phases: 4 frames per second for the first 3 seconds, then 2 frames per second for the next 3 seconds, and then 1 frame per second (0.5 frames per second in AlluraClarity) thereafter.

Image Analysis

The size of the lesion (largest dimension) was measured on an enhanced T1 image. The signal intensity of the lesion (caput medusa or umbrella-like draining vein) was visually assessed on SWI as either dark or high. ASL imaging was used to visually assess whether hyperintense signal was detected at the location where DVA or vpAVM was noted on contrast-enhanced imaging. In addition, ROIs were drawn in the most representative sections of the ASL quantitative CBF map (at the corresponding

location that matched the caput medusa or umbrella-like draining vein on the contrast-enhanced image) to determine the CBF of the DVA or vpAVM (CBF_{lesion}). To adjust for interindividual variation, we drew additional ROIs within the gray matter of normal contralateral parenchyma at the same section levels (CBF_{gray}). Subsequently, normalized CBF (nCBF) was calculated as $nCBF = CBF_{\text{lesion}} / CBF_{\text{gray}}$.¹³

Using DSA, we endeavored to quantify arteriovenous shunting using 2 different ways to measure the temporal phase in which the lesions were visualized. First, we calculated the delay between the first visualization of the intracranial artery (carotid genu in the anterior circulation, V4 segment of the vertebral artery in the posterior circulation) and the first appearance of the lesion (DVA or vpAVM). Hence, we used the following equation: Temporal Phase of the Lesion (TP, sec) = Timeframe of Appearance of the Lesion – Timeframe of Intracranial Artery Visualization. Second, the time of detection of the lesion was measured against the first visualization of the cortical vein (temporal phase in regard to the cortical vein [TCV]). The earlier appearance of the lesion was translated to a negative value. We evaluated the correlation between the nCBF and TP by calculating the Pearson correlation coefficient.

RESULTS

Both DSA and multiphase ASL images were available in 17 patients who had lesions with a caput medusa or umbrella-like appearance on contrast-enhanced MR imaging. Four patients were excluded due to comorbidities limiting normal intracranial perfusion; these included Moyamoya disease, stenotic intracranial vasculitis, severe carotid stenosis, and a dural AVF with severe cortical reflux. Clinical and lesion characteristics as well as imaging features are summarized in the Online Supplemental Data. At the time of DSA, 6 patients (cases 1–6) were diagnosed with 8 vpAVMs (2 lesions in cases 4 and 6), while 7 patients (cases 7–13) were diagnosed with DVAs. There were 7 men and 6 women, with a mean age of 46.4 years (range, 20–72 years) at the time of the ASL image acquisition.

Two patients diagnosed with vpAVM presented with hemorrhage (cases 1 and 3), while 4 patients presented with unrelated symptoms. Signs of intracranial hypotension (diffuse meningeal thickening, engorged dural sinus, and so forth) were observed on MR images of case 6. Seven lesions were detected during diagnostic work-up of various comorbidities (syncope in case 7, carotid disease in case 8, a separate AVM in cases 9 and 11, an unruptured aneurysm in cases 10 and 12, and a meningioma in case 13). Two patients presenting with hemorrhage (cases 1 and 3) underwent gamma knife surgery (GKS). In case 3, image analysis was performed on the residual vpAVM 3 years after the first GKS session. GKS was also performed for a separate AVM in cases 9 and 11. All patients remained event-free during the mean follow-up period of 73.9 months (median, 33 months; range, 3–571 months).

After meticulous analysis of the DSA images, we categorized study cases into 3 groups according to TP and TCV on DSA. The first group consisted of “typical vpAVM,” which showed the characteristic appearance of early venous drainage, with the TP of <2 seconds and negative-value TCV (cases 1–5). Lesions in the second group did not exhibit overt arteriovenous shunting

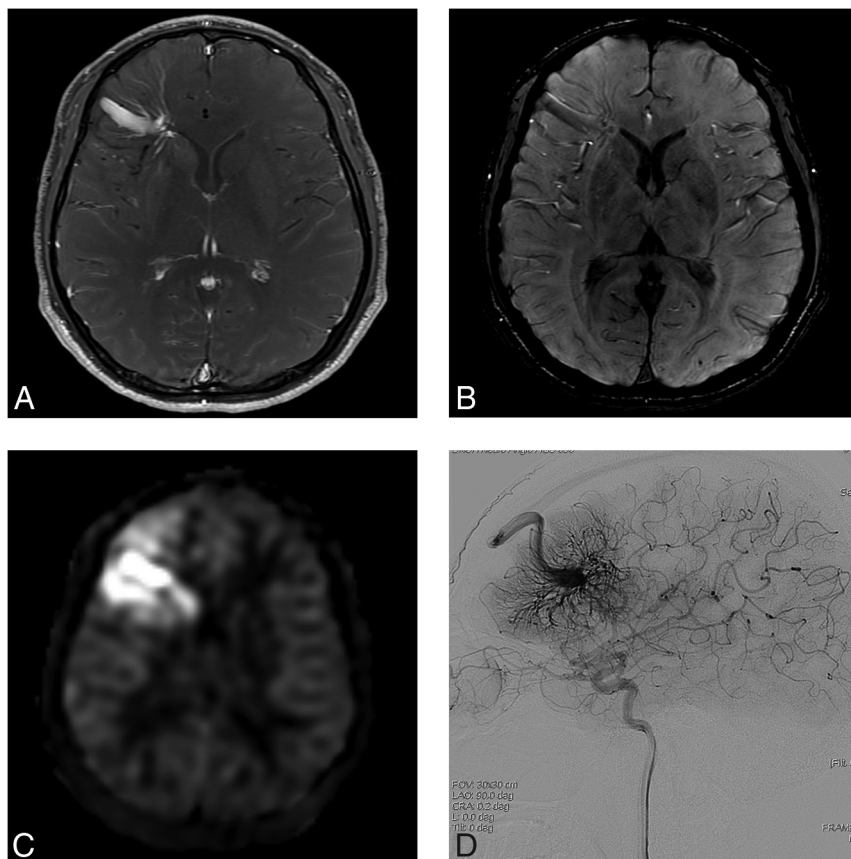


FIG 1. A 31-year-old man presenting with dizziness (case 4). A, Contrast-enhanced T1-weighted axial MR imaging shows a DVA-like lesion in the left frontal lobe. B, On SWI, both hyperintense and hypointense signal is present in the collecting vein, while only hypointense signal is present in the dilated medullary veins. C, The ASL quantitative CBF image demonstrates hyperintense signal intensity in the collecting vein and parenchyma corresponding to the location of the lesion, suggesting a vpAVM. D, On DSA, a caput medusae appearance of medullary veins draining to the superior sagittal sinus via a collecting cortical vein is visualized in the arterial phase.

and resembled DVAs. These lesions were first observed during the late capillary or early venous phase, deemed the “intermediate stage,” TP between 2.5 and 5 seconds and TCv between 0 and 3 seconds (cases 6 to 10). In the third group, lesions manifested themselves at the late venous phase with the appearance of a “classic DVA,” TP of >10 seconds and TCv of >5 seconds (cases 11–13).

It was evident that visually, ASL signal was markedly increased in the typical vpAVM group, while there was no discernible signal from lesions in the classic DVA group. In the intermediate group, however, 3 of 6 lesions (cases 6 [2 lesions] and 9) showed increased ASL signal; the other 3 lesions did not. Moreover, in those 3 lesions with increased ASL signal, the intensity was not as prominent as those observed in the typical vpAVM group. The nCBF was <2 in those 3 lesions from the intermediate group. The nCBF in the typical vpAVM group was >2, except in case 3, probably because a small residual portion of the lesion remained after GKS. Representative images from illustrative cases are shown in Figs 1–3.

The distribution of nCBF and TP values for the 3 groups of lesions is shown in Fig 4. The nCBF on ASL and TP on DSA were moderately negatively correlated across all groups: $r(13) = 0.66$, $P = .008$. On SWI, only 3 of 6 lesions in the typical vpAVM

group exhibited hyperintense signal in the dilated medullary veins, whereas all lesions in the intermediate and classic DVA groups had hypointense signal.

DISCUSSION

Detection of vpAVMs has become more frequent recently due to the increased availability of advanced imaging modalities. Various nomenclatures used to indicate vpAVM include transitional venous anomaly, DVA with an arterial component, and atypical DVA.^{6,14–16} Although the natural course of a vpAVM is poorly understood due to its low incidence, it is generally considered to carry a considerable risk of hemorrhage. Dilated medullary veins converging to a collecting vein is not infrequently encountered on enhanced MR imaging and is usually designated as a DVA in a routine clinical setting. Indeed, most of these lesions are DVAs; a previous study reported that only 8% of lesions with a DVA-like appearance on MR imaging showed increased ASL signal.¹⁷ Given that ASL is increasingly included as a regular sequence in MR imaging, we aimed to investigate the accuracy of ASL in distinguishing a vpAVM from a DVA.

Our study is the first to use DSA in study cases with DVA or vpAVM to fully validate ASL. The study results show the following: 1) A lesion with a

caput medusae appearance on contrast-enhanced MR imaging could be a vpAVM or DVA but could also be a lesion with intermediate shunting; and 2) ASL effectively predicts the presence of a vpAVM on MR imaging, and ASL signal intensity (nCBF) correlates well with how early the lesion appears on DSA (ie, the degree of arteriovenous shunting).

ASL imaging uses magnetically labeled water protons in arterial blood as an endogenous tracer to evaluate cerebral perfusion. Because there is no need for administration of a gadolinium-based contrast agent in dynamic susceptibility contrast-enhanced perfusion imaging, the risk of nephrogenic systemic fibrosis in patients with decreased renal function is nonexistent. As with an intracranial AVM, the utility of ASL in various other cerebrovascular conditions, including dural arteriovenous fistula, Moyamoya disease, and meningioma, has been well-documented.^{13,18,19} Most patients with cerebral vascular lesions in our institution currently undergo multiphase ASL. Multiphase ASL was initially introduced and used to evaluate perfusion in patients with stenotic lesions because the CBF value based on conventional ASL is underestimated due to the long arterial transit time. A previous study showed that the multiphase ASL technique can overcome the effect of delayed transit time on perfusion maps.¹² In nonstenotic vascular territory,

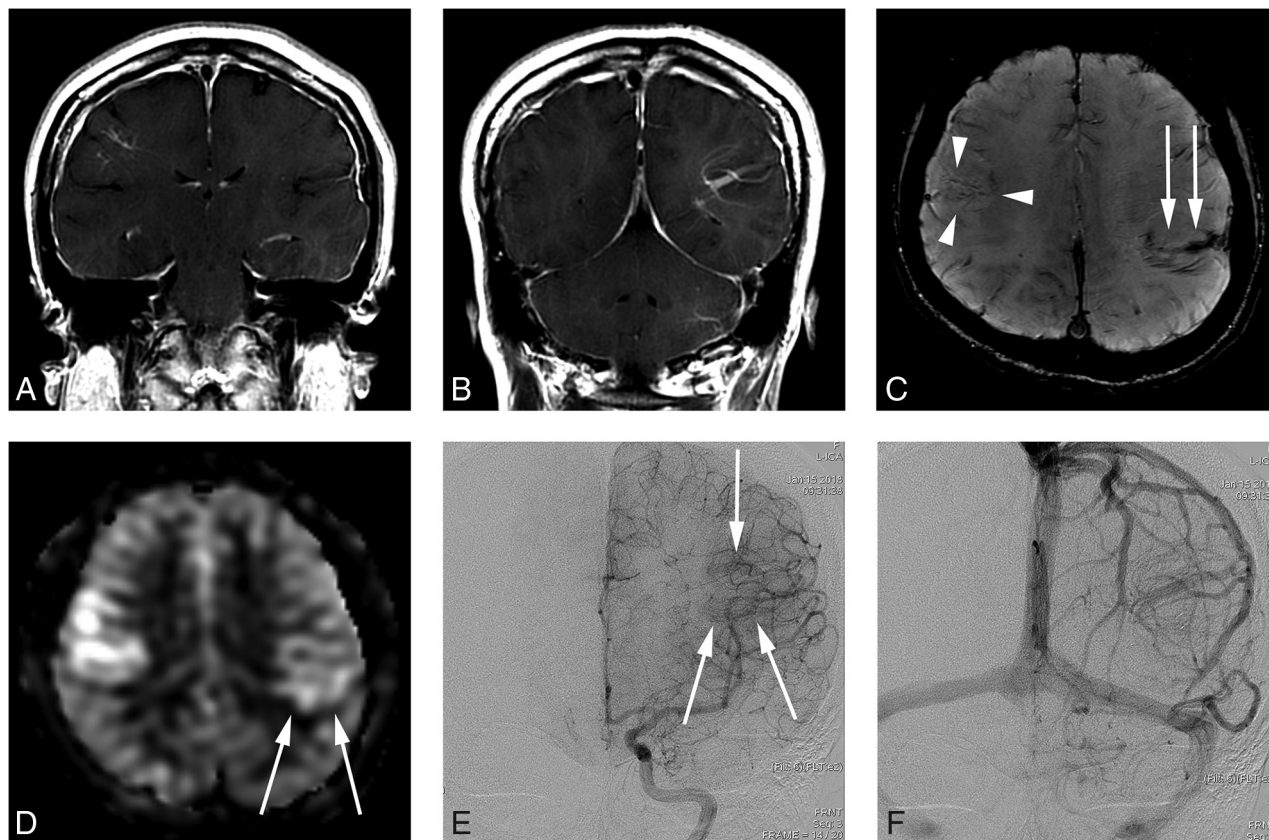


FIG 2. A 34-year-old woman presenting with a headache (case 6). *A* and *B*, Contrast-enhanced T1-weighted coronal MR imaging shows a DVA-like lesion in the bilateral parietal lobes. *C*, SWI demonstrates only hypointense signal in both the right (*arrowheads*) and left (*arrow*) lesions. *D*, The ASL quantitative CBF image demonstrates mildly hyperintense signal intensity in the parenchyma, corresponding to the location of the lesion. The left-sided lesion exhibits particularly subtle signal (*arrows*). *E*, In the late arterial phase of DSA, dilated medullary veins are gradually and subtly visualized (*arrows*). *F*, In the venous phase, dilated medullary veins draining to a collecting vein typical of a DVA are seen.

however, CBF values from both conventional and multiphase ASL showed high concordance levels with CBF values from DSC MR imaging. Therefore, although multiphase ASL may not be as widely used as conventional ASL, the findings from multiphase ASL in our study may well be applicable to conventional ASL.

Earlier studies have reported that arteriovenous shunting manifests as hyperintense signal intensity on SWI because arterial and venous circulation appear hyperintense (due to rapid flow) and hypointense (due to slow flow and deoxyhemoglobin), respectively.^{10,11} However, in 3 of 6 typical vpAVMs in our study, SWI indicated a DVA, with hypointense signal at the dilated medullary veins, though iso- to hyperintense signal could be detected at a stem vein in 2 cases. This finding suggests that ASL is capable of distinguishing a vpAVM from a DVA more accurately than SWI. The mechanism of how hypointense signal could be present in vpAVM (especially in such a high-flow lesion as in case 4, Fig 1) is not clear. It might be that some vpAVMs also drain normally circulated parenchymal venous flow, thus functioning as a DVA as well.⁶ The arteriovenous shunt flow may not be enough to rapidly wash out venous drainage in dilated medullary veins, resulting in hypointense signal from venous blood that is rich in deoxyhemoglobin.

Although lesions were clinically diagnosed as either DVAs or vpAVMs at the time of the DSA study, retrospective analysis of

DSA images for the present study indicated 3 distinct groups based on the degree of arteriovenous shunting. This finding suggests a spectrum of vascular malformations with varying hemodynamic characteristics, ranging from purely vein-draining DVAs to vpAVMs with overt arteriovenous shunting. This spectrum could possibly be explained by potential interrelation between DVAs and AVMs. It is well-known that DVAs and cavernous malformations commonly coexist, because venous hypertension and angiogenic proliferation caused by abnormal vascular anatomy of the DVA may lead to formation of the cavernous malformation.²⁰ Likewise, it is thought that thrombosis in venous radicles of a DVA may generate a fistula, similar to hypothetic dural arteriovenous fistula development, via various processes such as inflammation, venous hypertension, or angiogenesis.^{5,20}

The intermediate group lesions in our series may represent either lesions in the transitional stage from a DVA to a vpAVM or a vpAVM with progression of fistula formation terminated at a point of a low amount of shunting. The former supposition is supported by a case report in which previously nonexistent arteriovenous shunting developed into a DVA after 5 years.²¹ However, the possibility of the latter hypothesis cannot be completely excluded because there is no other report of a DVA developing into a vpAVM. In addition, follow-up ASL imaging was available in 3 cases in our study in which there was no evident change in ASL

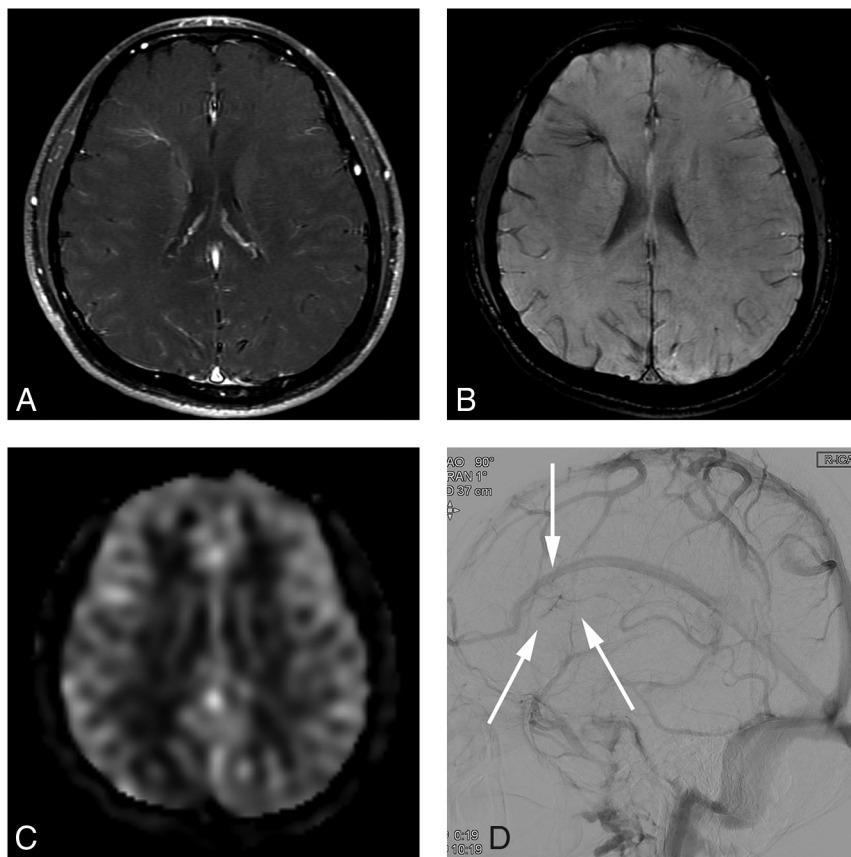


FIG 3. A 29-year-old man presenting with an AVM in the left occipital lobe (case 11). *A*, Contrast-enhanced T1-weighted axial MR imaging shows a DVA-like lesion in the right frontal lobe. *B*, SWI shows hypointense signal in the lesion. *C*, An ASL quantitative CBF image demonstrates no identifiable signal corresponding to the lesion. *D*, On DSA, the lesion is first visualized in the late venous phase (arrows), as is typically seen in a classic DVA.

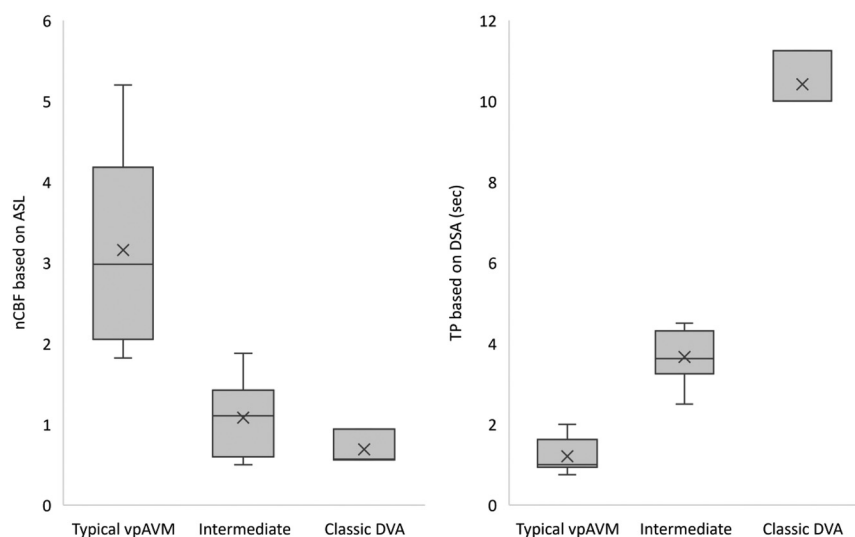


FIG 4. Box-and-whisker display of nCBF and TP for the 3 groups of lesions. The *line* across the boxes denotes the median value, whereas the *ends* of the boxes represent the first and third quartiles (not applied in the classic DVA group due to the small number of cases). The *ends* of each plot indicate the smallest and largest values. *x* denotes average value. Sec indicates second.

signal (1 in each group: case four, 36 months; case nine, 46 months; case thirteen, 4 months).

In any case, ASL imaging enabled instant visual detection of vpAVMs. In addition, our study results indicate that the nCBF effectively reflects the degree of arteriovenous shunting. The moderately negative correlation of $r(13) = 0.66$ between nCBF and TP on DSA may have been attenuated by the locational variation of DVAs. The nCBF of DVAs located near the cerebral cortex was measured to be near 1 due to normal cerebral perfusion, while the value was much lower (about 0.5) in DVAs located in deep cerebral matter.

Management strategies for a vpAVM are not well-established due to the small number of cases and paucity of data on treatment outcome. In cases of repetitive or extensive hemorrhagic lesions, surgical removal can be considered, though incomplete resection due to poor localization may lead to venous infarction or massive hemorrhage. In cases of symptomatic high-flow vpAVM, GKS may alleviate hemodynamic stress, though complete obliteration is seldom achieved.^{3,4} Endovascular treatment plays a limited role in vpAVMs because the lesions exhibit diffuse distribution without a definite dominant arterial feeder. De Maria et al⁵ have advocated conservative management, even in the presence of hemorrhage. They argued that hemorrhage is due to venous infarction by the thrombosis of one of the large collecting veins rather than the presence of a weak point in the vessels. It is generally accepted that conservative management will suffice for hemodynamically stable or asymptomatic lesions. In our case series, there was no bleeding in both hemorrhagic and nonhemorrhagic lesions during a relatively long follow-up period (mean, 73.9 months). Therefore, the clinical implication of an incidentally detected vpAVM is unclear. However, physicians should be aware of the possibility of a future hemorrhagic presentation and caution patients with vpAVMs about this. Meanwhile, in patients presenting with intracerebral hemorrhage by a ruptured vpAVM, ASL has the potential to suggest an

arteriovenous shunt in the initial work-up with MR imaging, even if a small lesion is partially obscured by mass effect from the hematoma.²²

There are some limitations to the present study primarily due to the retrospective nature of the study. First, DSA is not usually performed in patients with DVAs, and we were able to recruit only a small number of selected cases of DVAs in which DSA was performed to evaluate a separate disease. Therefore, our DVA cases are subject to nonrepresentative sampling and selection bias. Second, in cases of vpAVMs, a higher frame rate on DSA (eg, 7 frames per second) for the purpose of this study would have provided a more sensitive analysis of the shunt. However, only DSA images acquired with routine protocol were available.

Third, MRA was not evaluated in our study, though various MRA techniques could be used to detect arteriovenous shunt lesions. In our institution, contrast-enhanced MRA and 4D MRA were not routinely used; while TOF-MRA was mostly used in daily practice, the whole brain up to vertex was not covered. Future study comparing ASL and MRA sequences in detecting a vpAVM would produce more comprehensive results. Finally, analysis of ASL and DSA images depended on subjective and inconsistent visual assessment, without computerized measurement. Therefore, parameters such as the ROI drawn on ASL or the first appearance of the lesion or cortical vein on DSA are subject to slight inaccuracy. Despite these shortcomings, this study suggests that ASL has a clear role in screening overt vpAVMs in patients with dilated medullary veins converging to a collecting vein on contrast-enhanced MR imaging.

CONCLUSIONS

DVA and vpAVM are not readily discernible on contrast-enhanced or susceptibility-weighted MR imaging. ASL may predict the presence and amount of arteriovenous shunting in vpAVM, and using ASL enables confirmation of a vpAVM without DSA. However, the existence of a lesion with an intermediate amount of shunting should be considered. These lesions exhibit iso- or subtly increased signal on ASL, and their nature should be further investigated.

Disclosure forms provided by the authors are available with the full text and PDF of this article at www.ajnr.org.

REFERENCES

- Gokce E, Acu B, Beyhan M, et al. **Magnetic resonance imaging findings of developmental venous anomalies.** *Clin Neuroradiol* 2014;24:135–43 [CrossRef Medline](#)
- Aoki R, Srivatanakul K. **Developmental venous anomaly: benign or not benign.** *Neurol Med Chir (Tokyo)* 2016;56:534–43 [CrossRef Medline](#)
- Im SH, Han MH, Kwon BJ, et al. **Venous-predominant parenchymal arteriovenous malformation: a rare subtype with a venous drainage pattern mimicking developmental venous anomaly.** *J Neurosurg* 2008;108:1142–47 [CrossRef Medline](#)
- Jeon JP, Kim JE, Ahn JH, et al. **Long-term treatment outcome of venous-predominant arteriovenous malformation.** *J Neurosurg* 2016;124:1100–06 [CrossRef Medline](#)
- De Maria L, Lanzino G, Flemming KD, et al. **Transitional venous anomalies and DVAs draining brain AVMs: a single-institution case series and review of the literature.** *J Clin Neurosci* 2019;66:165–77 [CrossRef Medline](#)
- Picart T, Dumot C, Guyotat J, et al. **Arteriovenous malformation drained into a developmental venous anomaly: a case report and up-dated literature review.** *Neurochirurgie* 2020;66:471–76 [CrossRef Medline](#)
- Haller S, Zaharchuk G, Thomas DL, et al. **Arterial spin labeling perfusion of the brain: emerging clinical applications.** *Radiology* 2016;281:337–56 [CrossRef Medline](#)
- Sunwoo L, Sohn CH, Lee JY, et al. **Evaluation of the degree of arteriovenous shunting in intracranial arteriovenous malformations using pseudo-continuous arterial spin labeling magnetic resonance imaging.** *Neuroradiology* 2015;57:775–82 [CrossRef Medline](#)
- Kodera T, Arai Y, Arishima H, et al. **Evaluation of obliteration of arteriovenous malformations after stereotactic radiosurgery with arterial spin labeling MR imaging.** *Br J Neurosurg* 2017;31:641–47 [CrossRef Medline](#)
- Jagadeesan BD, Delgado Almandoz JE, Moran CJ, et al. **Accuracy of susceptibility-weighted imaging for the detection of arteriovenous shunting in vascular malformations of the brain.** *Stroke* 2011;42:87–92 [CrossRef Medline](#)
- Hodel J, Leclerc X, Kalsoum E, et al. **Intracranial arteriovenous shunting: detection with arterial spin-labeling and susceptibility-weighted imaging combined.** *AJNR Am J Neuroradiol* 2017;38:71–76 [CrossRef Medline](#)
- Yun TJ, Sohn CH, Yoo RE, et al. **Transit time corrected arterial spin-labeling technique aids to overcome delayed transit time effect.** *Neuroradiology* 2018;60:255–65 [CrossRef Medline](#)
- Yoo RE, Yun TJ, Cho YD, et al. **Utility of arterial spin labeling perfusion magnetic resonance imaging in prediction of angiographic vascularity of meningiomas.** *J Neurosurg* 2016;125:536–43 [CrossRef Medline](#)
- Oran I, Kiroglu Y, Yurt A, et al. **Developmental venous anomaly (DVA) with arterial component: a rare cause of intracranial haemorrhage.** *Neuroradiology* 2009;51:25–32 [CrossRef Medline](#)
- Roh JE, Cha SH, Lee SY, et al. **Atypical developmental venous anomaly associated with single arteriovenous fistula and intracerebral hemorrhage: a case demonstrated by superselective angiography.** *Korean J Radiol* 2012;13:107–10 [CrossRef Medline](#)
- Zhang M, Telischak NA, Fischbein NJ, et al. **Clinical and arterial spin-labeling brain MRI features of transitional venous anomalies.** *J Neuroimaging* 2018;28:289–300 [CrossRef Medline](#)
- Iv M, Fischbein NJ, Zaharchuk G. **Association of developmental venous anomalies with perfusion abnormalities on arterial spin-labeling and bolus perfusion-weighted imaging.** *J Neuroimaging* 2015;25:243–50 [CrossRef Medline](#)
- Amukotuwa SA, Marks MP, Zaharchuk G, et al. **Arterial spin-labeling improves detection of intracranial dural arteriovenous fistulas with MRI.** *AJNR Am J Neuroradiol* 2018;39:669–77 [CrossRef Medline](#)
- Lee S, Yun TJ, Yoo RE, et al. **Monitoring cerebral perfusion changes after revascularization in patients with moyamoya disease by using arterial spin-labeling MR imaging.** *Radiology* 2018;288:565–72 [CrossRef Medline](#)
- Aboian MS, Daniels DJ, Rammos SK, et al. **The putative role of the venous system in the genesis of vascular malformations.** *Neurosurg Focus* 2009;27:E9 [CrossRef Medline](#)
- Pilipenko Y, Konovalov A, Okishev D, et al. **Formation during lifetime of arteriovenous shunt in developmental venous anomaly that caused intracerebral hemorrhage.** *World Neurosurg* 2018;119:168–71 [CrossRef Medline](#)
- Hak JF, Boulouis G, Kerleroux B, et al. **Arterial spin-labeling for the etiological workup of intracerebral hemorrhage in children.** *Stroke* 2022;53:185–93 [CrossRef Medline](#)